TELKOMNIKA, Vol.17, No.2, April 2019, pp.995~1005
ISSN: 1693-6930, accredited First Grade by Kemenristekdikti, Decree No: 21/E/KPT/2018
DOI: 10.12928/TELKOMNIKA.v17i2.8616

A high efficiency BPSK receiver for short range wireless network

Mousa Yousefi*[1], Khalil Monfaredi[2]
Department of Electrical Engineering, Faculty of Engineering,
Azarbaijan Shahid Madani University, Tabriz, Iran
*Corresponding author, e-mail: m.yousefi@azaruniv.ac.ir[1], khmonfaredi@azaruniv.ac.ir[2]

Abstract

In this paper, a 910MHz high efficiency BPSK receiver is presented with Colpitts oscillator for short range wireless network. In this research, with injection-lock technique and using Colpitts oscillator, the efficiency of receiver has been improved. And also, behavior of an oscillator under injection of another signal has been investigated. Also, variation of output signal amplitude versus injected signal phase variation, the effect of varying the amplitude of injected signal and quality factor of the oscillator has been investigated. The designed receiver has 0.474 mW dc power and -60 dBm sensitivity. Data rate of receiver is 5 Mbps. The FOM of receiver is 94 pJ/bit. This receiver was designed and simulated in 0.18 µm RFCMOS technology. This proposed receiver can be used in short range wireless network for example, Wireless Body array network and wireless sensor network.

***Keywords**: BPSK, network, receiver, short, wireless*

1. Introduction

Transceivers for wireless sensor network have lately spurred lots of researches and developments [1]. Energy consumption of transceiver block of wireless sensor network must be as low as possible like all other block of the system [2, 3]. Short Range Wireless Network contains WBSN, WSN and etc [4]. WBSN contain personal serves and sensors that displaying of biotic signals. Personal serves composed of mobile phone, personal computer, internet, laptop and WLAN that it connects medical center and WBSN [5-14].

Distance between sensor node and central node is 3 meter. For this reason, required output power must be less than 1 mW [15]. Sensor node is combined of sensing part, analog to digital converter (ADC), microprocessor, and transceiver [16-19]. The transceiver is a block with higher power consumption between other blocks, for this reason, design of transceiver of short range wireless is challenging [20, 21]. Typically, Low power transceivers use modulations such as OOK, FSK, or PSK. The choice of modulation affects to overall radio frequency system [22]. The OOK offers the low power solution because demodulation does not need an accurate reference signal [11]. Albeit an OOK modulation system uses low power in the receiver part, it is rarely used due to low data rates associated with high settling times and increased sensitivity to interferers [6, 23-25].

BPSK modulation is preferred for transceiver because of its better noise immunity [26]. BPSK modulation needs to complex system for detecting radio frequency signal but with using of injection lock technique can be used simple system for demodulation [27]. Thus, with used of injection-locked technique can be decreased power consumption. In the typical, Figure of merit for receiver is that how much energy is needed for detection one bit. FOMRX has units of J/(bit). In order to increase the life time wireless systems, data rate and dc power must be high and low respectively. High data rate wireless is required for medical applications [20, 21]. In this paper, high efficiency BPSK receiver is proposed with injection lock technique. Main operation of proposed receiver is described in the Section 2. Simulation results are presented in section 3. Eventually, in section 4, conclusion of paper is made.

Received January 16, 2018; Revised December 25, 2018; Accepted January 10, 2019

2. The Proposed Architecture

In the designed receiver, BPSK modulation is utilized, in which binary ‘1’ is represented by phase 0 and binary ‘0’ is represented by phase 180^0. The receiver is composed of several blocks: the LO generation, ADC, envelop detector and the LNA and transmitter section composed of oscillator and power amplifier. The block diagram receiver is represented by Figure 1.

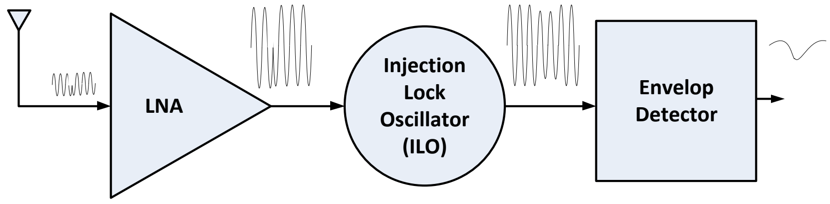

Figure 1. Block diagram of receiver

2.1. Injection-lock Receiver

For simple investigation of injected signal behavior on the oscillator, consider Figure 2. In this paper, the structure of an oscillator with feedback has been shown. A phase difference of 180 degree is generated in feedback path. Applying the injected signal generates an additional phase difference in feedback path. θ_0 is the phase difference of the injected signal.

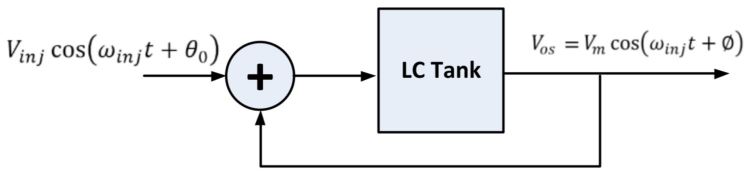

Figure 2. Block diagram of an oscillator with injection signal

To keep the oscillations, the oscillator omits the generated phase difference. In this condition, the frequency of the oscillator changes for free-running frequency (with this assumption that injected frequency is in locking bandwidth of injection lock. As shown in Figure 1, output voltage after adding injected signal and oscillator output signal is:

$$V_x = V_{inj}\cos(\omega_{inj}t+\theta_0) + V_{os}\cos(\omega_{inj}t+\theta_0) \quad (1)$$

$$V_x = A\cos(\omega_{inj}t) - B\cos(\omega_{inj}t) \quad (2)$$

In equation above, equals $V_{inj}\cos\theta_0+V_{os}\cos\theta$, B equals $V_{inj}\sin\theta_0+V_{os}\sin\theta$, V_{inj} is the amplitude of the injected signal, V_{os} is the amplitude of the oscillator output signal and Q is the quality factor of the oscillator. Voltage V_x, can be expressed as sine signal:

$$V_x = V_m\cos(\omega_{inj}t+\emptyset) \quad (3)$$

In (3), φ equals $\tan^{-1}$(B/A), V_m equals ($v_{inj}^2+Vos^2+2V_{inj}V_{os}(\sin\theta_0\sin\theta+\cos\theta\cos\theta_0)$). Noting that, V_{inj}<<V_{os} equation for V_x can be simplified as follows:

if signal V_x is passed through an LC tank, the output voltage will be:

$$V_{os} \approx V_m\cos(\omega_{inj}t+\emptyset) \quad (4)$$

If we equate (3) with output of the oscillator, it can be seen that:

$$V_{out} = V_m \cos\left(\omega_{inj} t + \varphi + tan^{-1}(\omega_0 - \omega_{inj} - \frac{d\varphi}{dt})\right) \quad (5)$$

if we calculate the derivative of 6:

$$\varphi + tan^{-1}\left(\omega_0 - \omega_{inj} - \frac{d\varphi}{dt}\right) = \theta \quad (6)$$

As the injected signal has smaller amplitude in comparison to the output signal of the oscillator, equation can be approximated as:

$$\frac{d\varphi}{dt} = \frac{V_{os}^2 + V_{os} V_{inj}(sin\theta_0 sin\theta + cos\theta cos\theta_0)}{V_{os}^2 + V_{inj}^2 + 2V_{os} V_{inj}(sin\theta_0 sin\theta + cos\theta cos\theta_0)} \cdot \frac{d\theta}{dt} \quad (7)$$

using trigonometry relationships

$$\frac{d\varphi}{dt} \approx \frac{d\theta}{dt} \quad (8)$$

with approximating in (9):

$$\tan(\theta - \varphi) = \frac{V_{inj}(sin\theta_0 sin\theta + cos\theta cos\theta_0)}{V_{os} + V_{inj}(sin\theta_0 sin\theta + cos\theta cos\theta_0)} \quad (9)$$

$$\tan(\theta - \varphi) = \frac{V_{inj}(sin\theta_0 sin\theta + cos\theta cos\theta_0)}{V_{os}} \quad (10)$$

the following result can be achieved:

$$\frac{d\theta}{dt} = \omega_0 - \omega_{inj} - \frac{\omega_0 V_{inj}}{2QV_{os}} \sin(\theta - \theta_0) \quad (11)$$

If the frequency of injected signal is within the bandwidth locking can be achieved. This range is given by (12) based on discussion and analyses

$$\omega_L = \frac{\omega_0 V_{inj}}{2QV_{os}} \quad (12)$$

in (11) can be rewritten by using:

$$\frac{d\theta}{dt} = \omega_0 - \omega_{inj} - \omega_L \sin(\theta - \theta_0) \quad (13)$$

The time interval which is required for oscillator to be stable after signal injection or in the other words, locked is called locking time. After locking time, phase does not change anymore ($d\varphi/dt=0$), so:

$$\varphi = sin^{-1}(\frac{\omega_0 - \omega_{inj}}{\omega_L}) \quad (14)$$

after phase difference generation in injected signal, locking condition is reached again. Final phase difference after locking, θ2 can be achieved from 14:

$$\theta_2 - \theta_0 = sin^{-1}(\frac{\omega_0 - \omega_{inj}}{\omega_L}) \quad (16)$$

before locking, structure was in locking condition and output signal phase difference with injected signal is equal to:

$$\theta_2 = \theta_1 + \theta_0 \tag{17}$$

so from 17, it can be seen that with generating phase difference in injected signal, output signal will have equal phase difference with injected signal.

$$\theta_1 = sin^{-1}(\frac{\omega_0-\omega_{inj}}{\omega_L}) \tag{18}$$

2.2. Analysis of Injected Signal Phase Change on Locking Time

Analysis of locking time when the phase of injected signal changes is investigated in the following in (13) can be rewritten as:

$$dt = \frac{d\varphi}{\omega_0-\omega_{inj}-\omega_L\sin(\varphi)} \qquad (18)$$

$$\sin(\varphi) = \frac{2\tan(\varphi/2)}{1+tan^2(\varphi/2)} \tag{19}$$

using variable change u=tan(φ/2) and with the assumption that the frequency of injected signal is within the bandwidth of injection-lock:

$$\alpha\omega_L = \omega_0 - \omega_{inj} \quad 0<\alpha<1 \tag{20}$$

replacing in the equations above:

$$\frac{d\varphi}{\omega_L(\alpha-sin(\varphi))} = dt \tag{21}$$

equation can be written as:

$$\frac{2}{\alpha\omega_L}\frac{du}{u^2-\frac{2u}{\alpha}+1} = dt \tag{22}$$

$$\frac{2du/\alpha\omega_L}{(u-u_1)(u-u_2)} = dt \tag{23}$$

$$u_{1,2} = \frac{1}{\alpha} \mp \sqrt{\frac{1}{\alpha^2} - 1} \tag{24}$$

using differential equations:

$$u = \frac{u_1-u_2Ke^{t/}}{1-Ke^{t/K_1}} \tag{25}$$

with initial condition at t=0, phase difference is equal to θ_1.

$$\frac{u_1-Ku_2}{1-K} = \tan(\frac{\theta_1-\theta_0}{2}) \tag{26}$$

$$K = \frac{\tan\left(\frac{\theta_1-\theta_0}{2}\right)-u_1}{\tan\left(\frac{\theta_1-\theta_0}{2}\right)-u_2} \tag{27}$$

the rate of phase variation at t→∞ is equal to 0. So:

$$\tan(\theta_2) = u_2 \tag{28}$$

In this section, we assume that an oscillator with resonance, ω_0 is stimulated with a signal frequency of, ω_{inj} and because the injected signal frequency is within locking bandwidth, oscillator has been locked. If in this condition, the phase of the injected signal changes, the free-running phase must vary to be able to lock again. With this comments, Equation is true for this condition, too. So the time interval for locking condition can be calculated from:

$$t = k_1 Ln(-\frac{53}{u_2 k} + \frac{25u_1}{u_2 k} + 25 \mp \sqrt{\left(-\frac{53}{u_2 k} + \frac{25u_1}{u_2 k} + 25\right) - 4\frac{u_1}{u_2 k}}) \quad (29)$$

2.3. LNA and Amplifier

In the Figure 3 the LNA transistor level schematic is shown. Low Noise Figure, high gain, good linearity, good matching and low power LNA is a requirement for the receiver. The LNA uses common source structure with cascode transistor. The L_1 and C_1 are used for input impedance matching with impedance of antenna (50 ohm) and filtering input signal. The common source stage of LNA is realized for amplifying, also, the cascode transistor M_2 is used to isolate antenna from load. As shown in Figure 3 the capacitor C3 serves as a dc block. For tuning the overall gain of LNA block, an inverter with resistive feedback has been used. In the proposed transceiver, the designed LNA has 280 µW dc power and -30 dB S_{11}.To maintain operating frequency, range of receiver with minimum input power, the LNA gain should be high enough. The proposed LNA has 40 dB variable voltage gain which can be adjusted by 4 digital signals. Finally, the output voltage of LNA is injected to current source of the oscillator.

2.4. Injection Locked Oscillator

Injection locked oscillator is the block that play a key role in the proposed receiver. A schematic of proposed injection locked oscillator is illustrated in Figure 4. The incident signal is injected on the gate terminal of transistor M2.

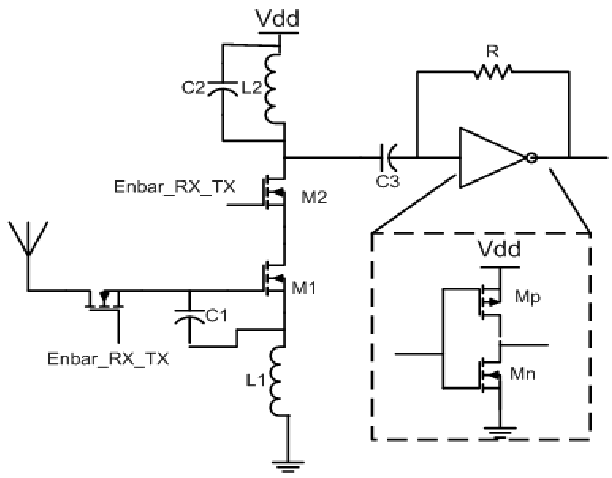

Figure 3. Low noise amplifier of receiver

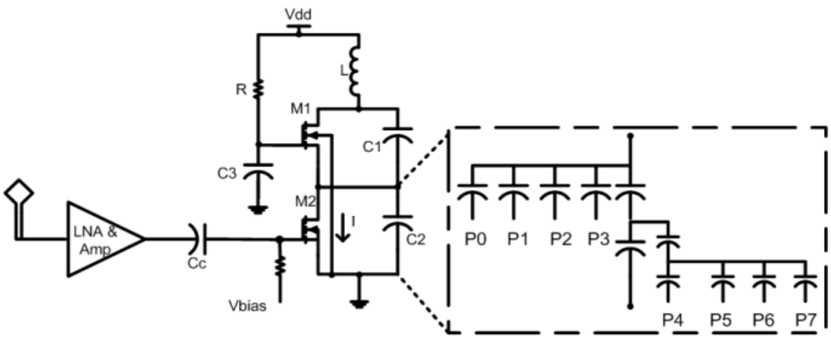

Figure 4. A schematic of colpitts oscillator

2.5. Envelop Detector

The envelop detector composed of one transistor with diode connection, resistor and capacitance. The resistor and capacitor act as a low pass filter. The envelop detector noise has a negligible effect on noise Figure of the receiver. The amplitude of envelop detector is detectable. In the following envelop detector; the common source amplifier is used. The envelop detector and common source are used to convert amplitude-modulated signal to DC baseband signal. The output signal of envelop detector section converted to 1-bit data with a digital convertor.

3. Results and Simulations

As an example, the effect of phase difference of the injected signal has been investigated in a typical LC oscillator See Figure 5. Table 1 is shown values of the components. In Figure 6 the output signal of the peak detector versus the frequency of injected signal has been illustrated. Figure 7 shows the output of the peak detector for 180 degrees phase with 2.4 GHz frequency. Also, in Figure 8 the effect of phase change of the injected signal versus frequency has been shown. Peak detector output has a lot of variation until locking again for 180-degree difference phase. Also, the locking time for oscillator to lock again, depends on phase difference and the amplitude of the injected signal. In Figure 8 locking time for different phases at three amplitude values of the injected signal has been shown. In this Figure 9 locking time decreases as the amplitude of the injected signal increases.

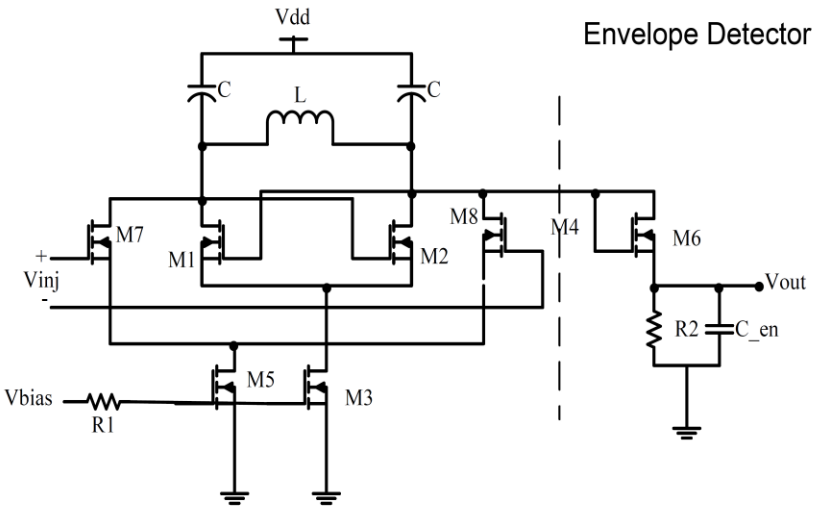

Figure 5. The circuitry of the oscillator

Table 1. Values of the Components used in Typical Oscillator

Device	Value	Device	Value	Device	Value
M1	W/L=80/0.18	Vbias	0.5v	C	7pF
M2	W/L=80/0.18	R1	10KΩ	C_en	20pF
M3	W/L=240/0.18	R2	80KΩ	L	6nH
M4	W/L=20/0.18	Vdd	2 V		

With using analysis above section, a receiver that used injection lock phenomenal is designed. The oscillator has a 910 MHz output signal with minimum 0.4 V swing. In the Table 2 is represented summary of proposed transceiver characteristics. Figure 10 shows that the oscillator has -160 dBc/Hz phase noise, while consuming 377 µA from 0.7 V power supply. In the Figure 11 waveform of received signal pattern and output envelop detector are shown with ‘1010’ data message and 5 Mbps data rate. The peak output voltage of envelop detector in ‘0’ and ‘1’ is 36 mV.

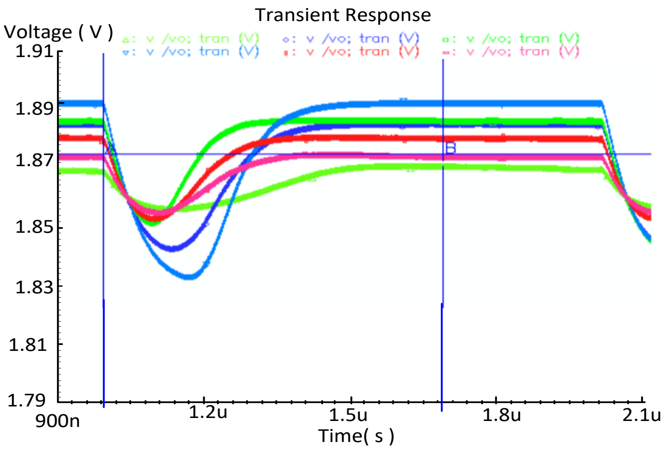

Figure 6. Time response of the oscillator under injection after injected signal phase change versus different frequencies.

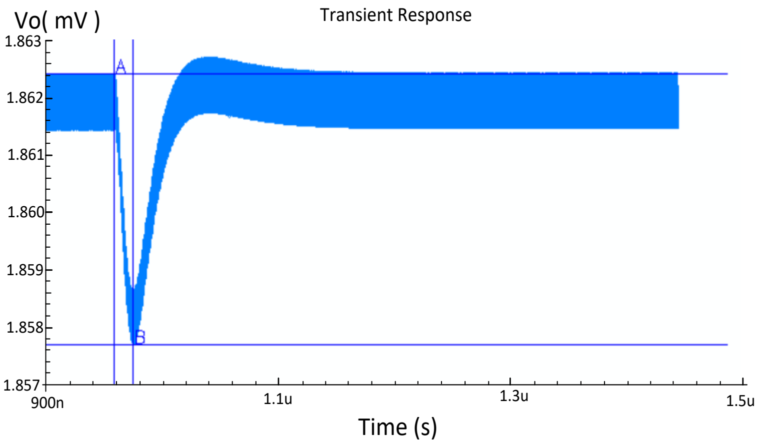

Figure 7. Time response of the oscillator under injection versus 180 phase change

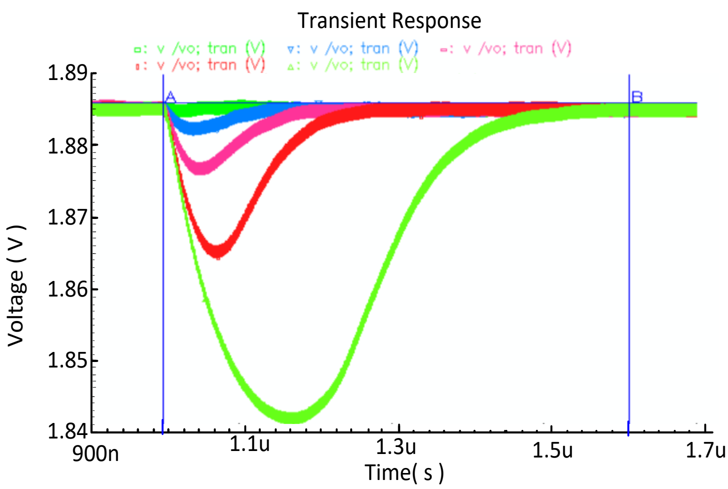

Figure 8. Time response of the oscillator under injection for different phase changes of injected signals at a specific frequency of 2.4 GHz

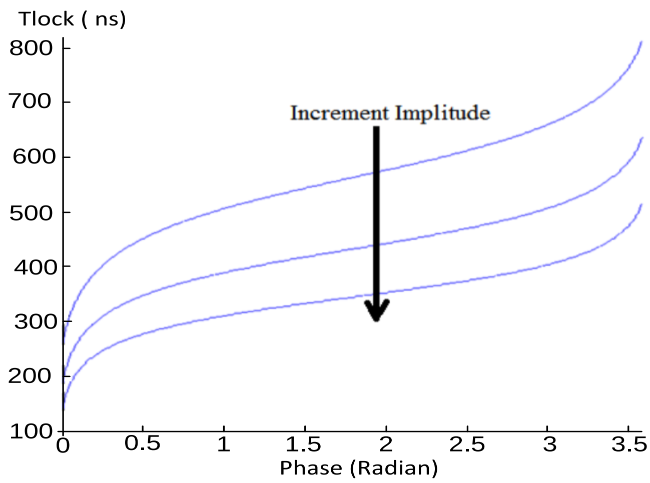

Figure 9. Time interval for locking again for half period of phase changes versus different amplitudes of the injected signal

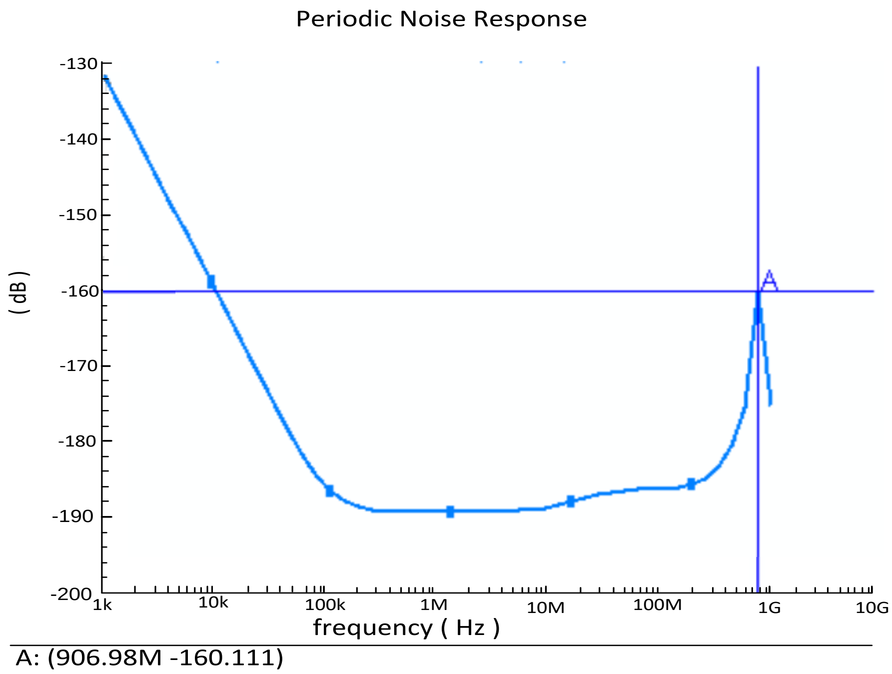

Figure 10. Phase nosie of oscillator

Table 2. Summary of the Proposed Receiver Characteristics

Parameters	Value
Power supply	0.7 V
Technology	0.18 µm
Modulation	BPSK
Maximum Data Rate	5 Mb/s

Figure 12 plots the DCO frequency with digital control signals. The DCO frequency can be tuned to a desired frequency over the range of 900 to 910 MHz. In fine calibration, frequency steps are nonlinear. The accuracy of DCO is maximum 100 kHz per one bit and also, for some steps, step of altering frequency is under 100 KHz. With 5 Mbps data rate and 8-bit control signal the required time for calibration is 50 µs. This calibration time is suitable in WBSN. In the Table 3 characteristics of different receivers are shown. All elements of the proposed transceiver are on chip elements expect the inductor of the oscillator. If all inductors are designed off chip (High Q) the FOM of the transceiver could better than the proposed transceiver. But the proposed transceiver consumes smaller area with favorable performance.

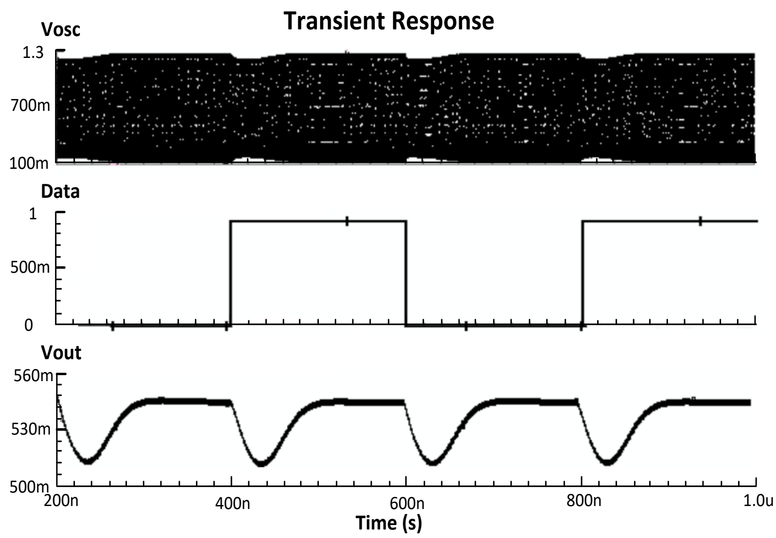

Figure 11. Waveform of data message with '1010' pattern and 5 Mbps data rate frequency

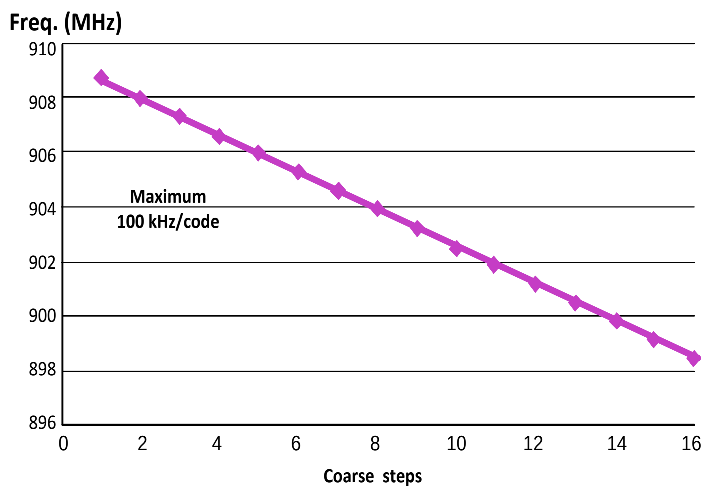

Figure 12. Frequency tuning curve of DCO

Table 3. The Performance Comparison of Receivers

Ref.	[6]	[28]	[29]	This work(sim.)
F_{RF}(GHz)	0.915/0.868	2.4	1.9	0.91
Sen. (dBm)	-50	-82	-31	-60
Pdc_{RX} (mW)	0.216	0.166	2.5	0.474
FOM_{RX} (pJ/bit)	108	332	250	94
Tech. (µm)	0.9	0.65	0.9	0.18
DR(Mbps)	2	0.5	10	5
Modulation	BPSK	OOK	BFSK	BPSK

4. Conclusion

In this paper, a highly efficient BPSK transmitter has been proposed for short range wireless network and analyzed injection lock technique with changing phase of injection signal. FOMRX is 94 pJ/(bit×mW). In the proposed receiver, colpitts oscillator has been used to generate RF carrier. The proposed receiver employs injection lock technique which decreases DC power of the receiver. All elements of the proposed transceiver are on chip elements expect the inductor of the oscillator.

References

[1] Goldsmith, A., *Wireless communications*. 2005: Cambridge university press.
[2] Ataeifard AK, Monfaredi S, Hossinzadeh. *Design and Simulation of Digitally Tuned Class C Voltage Controlled Oscillator with Enhanced Phase Noise Characteristics.* Tabriz Journal of Electrical Engineering, 2018. 48(2): 815-823.
[3] Monfaredi K. Distributed Unique-Size MOS Technique: A Promising Universal Approach Capable of Resolving Circuit Design Bottlenecks of Modern Era. *Circuits, Systems, and Signal Processing.* 2019; 38(2): 512-528.
[4] Aminian M, HR Naji. A hospital healthcare monitoring system using wireless sensor networks. *J. Health Med. Inform*. 2013; 4(2): 121.
[5] Wong AC, et al. *A 1V, micropower system-on-chip for vital-sign monitoring in wireless body sensor networks*. in *Solid-State Circuits Conference, 2008. ISSCC 2008. Digest of Technical Papers. IEEE International*. 2008. IEEE.
[6] Yan H, et al. An ultra-low-power BPSK receiver and demodulator based on injection-locked oscillators. *IEEE Transactions on Microwave Theory and Techniques*. 2011. 59(5): 1339-1349.
[7] Ayers JK, Mayaram, TS Fiez. *A low power BFSK super-regenerative transceiver*. in *Circuits and Systems, 2007. ISCAS 2007. IEEE International Symposium on*. 2007. IEEE.
[8] Otis B, YH Chee, J Rabaey. *A 400/spl mu/W-RX, 1.6 mW-TX super-regenerative transceiver for wireless sensor networks*. in *Solid-State Circuits Conference, 2005. Digest of Technical Papers. ISSCC. 2005 IEEE International*. 2005. Citeseer.
[9] Muhammad Anwar AHA, Kashif Naseer Qureshi, Abdul Hakeem Majid. Wireless Body Area Networks for Healthcare Applications: An Overview. *TELKOMNIKA Telecommunication Computing Electronics and Control*. 2017; 15(3): 1088-1095.
[10] ES A. Wearable Conformal Antennas for 2.4 GHz Wireless Body Area Networks. *TELKOMNIKA Telecommunication Computing Electronics and Control.* 2013. 11(1): 175-180.
[11] Yousefi M, et al. A–5 dBm 400MHz OOK Transmitter for Wireless Medical Application. *International Journal of Electronics and Telecommunications*. 2014; 60(2): 193-198.
[12] Yousefi M, et al. A 430 MHz fully integrated high efficiency OOK transmitter for wireless biomedical application. *International Journal of Electrical & Computer Sciences.* 2014; **4**: 1-5.
[13] Laneman JN, GW Wornell. *Energy-efficient antenna sharing and relaying for wireless networks*. in *Wireless Communications and Networking Confernce, 2000. WCNC. 2000 IEEE*. 2000. IEEE.
[14] Pashaei H, K Monfaredi. ROM-Less Fully Digital Synthesizer Design, Based on Novel phase to Sinusoidal Interface. *Journal of Telecommunication, Electronic and Computer Engineering (JTEC).* 2017: 9(3): 155-161.
[15] Savvides A, C.-C Han, MB Strivastava. Dynamic fine-grained localization in ad-hoc networks of sensors. in Proceedings of the 7th annual international conference on Mobile computing and networking. 2001. ACM.
[16] Yousefi M, Z Koozehkanani, J Sobhi. A 910MHz Injection Locked BFSK Transceiver for Wireless Body Sensor Network Using Colpitts Oscillator. *Journal of Iranian Association of Electrical and Electronics Engineers*. 2018. 14(4): 63-69.
[17] Azhari SJ, K Monfaredi, S Amiri. A 12-bit, low-voltage, nanoampere-based, ultralow-power, ultralow-glitch current-steering DAC for HDTV. *International Nano Letters.* 2012. 2(35): 1-7.
[18] Van't Hof J, DD Stancil. *Ultra-wideband high data rate short range wireless links*. in *Vehicular Technology Conference, 2002. VTC Spring 2002. IEEE 55th*. 2002. IEEE.
[19] Farsi, M.R. and K. Monfaredi. Design and Simulation of High Precision Second-order Sigma-delta Modulator for Bluetooth Applications. *Journal of Engineering Science and Technology.* 2018. 13(10): 3071-3079.
[20] Kamble J, I Pasha, M Madhavilatha. FPGA Implementation of Digital Modulation Technique for HRR Target Detection. *Indian Journal of Science and Technology.* 2015: 8(24): 1-6.
[21] Kosari A, M Moosavifar, DD Wentzloff. *A 152μW− 99dBm BPSK/16-QAM OFDM Receiver for LPWAN Applications*. *in 2018 IEEE Asian Solid-State Circuits Conference (A-SSCC).* 2018. IEEE.
[22] Sarkar K, T Kanjilal, S Basu. A Review on BPSK Modulation Techniques and Demodulation Schemes. *International Journal on Emerging Trends in Electronics & Communication Engineering*. 2018. 2(2).

[23] Bohorquez JL, AP Chandrakasan, JL Dawson. A 350$\mu $ W CMOS MSK Transmitter and 400$\mu $ W OOK Super-Regenerative Receiver for Medical Implant Communications. *IEEE Journal of Solid-state circuits*. 2009. 44(4): 1248-1259.

[24] Safaric S, K Malaric. *ZigBee wireless standard*. in *Multimedia Signal Processing and Communications, 48th International Symposium ELMAR-2006 focused on*. 2006. IEEE.

[25] Proakis JG. *Digital signal processing: principles algorithms and applications*. 2001: Pearson Education India.

[26] Tomkins A, et al. A zero-IF 60 GHz 65 nm CMOS transceiver with direct BPSK modulation demonstrating up to 6 Gb/s data rates over a 2 m wireless link. *IEEE Journal of Solid-state circuits.* 2009; 44(8): 2085-2099.

[27] Tang DD. *Microwave subcarrier generation for fiber optic systems*. 1991, Google Patents.

[28] Macias-Montero J, et al. *A 19GHz, 250pJ/bit non-linear BPSK demodulator in 90nm CMOS*. in *ESSCIRC, 2009. ESSCIRC'09. Proceedings of*. 2009. IEEE.

[29] Drago S, et al. *A 2.4 GHz 830pJ/bit duty-cycled wake-up receiver with−82dBm sensitivity for crystal-less wireless sensor nodes*. in *Solid-State Circuits Conference Digest of Technical Papers (ISSCC), 2010 IEEE International*. 2010. IEEE.